

PET Quantification Inaccuracy of Non-Uniform Tracer Distributions for Radiation Therapy

Assen S. Kirov, *Member, IEEE*, Christopher Danford, C. Ross Schmidlein, Ellen Yorke, John L. Humm, and Howard I. Amols

Abstract—The quantitative accuracy of PET has been measured for phantoms containing uniform activity spheres and cylinders, but has never been studied for non-uniformly varying tracer concentration (TC) distributions. For the correct delineation of tumors for radiation therapy (RT) using PET, the combined effect of all PET image degrading factors for realistic cases needs to be known.

We investigate PET inaccuracy for a phantom with TC and attenuation varying non-uniformly in one direction. This 1D model enables determination of the positional, angular and statistical effects on the quantification accuracy. We simulated a cylindrical uniform TC phantom containing a non-uniform TC insert using the GATE (Geant4 Application for Tomographic Emission) Monte Carlo code. The insert is made of thin parallel slabs with different TC, atomic composition and density. The phantom is simulated inside a validated model of the GE Discovery LS PET/CT scanner. The Software for Tomographic Image Reconstruction (STIR) was used to reconstruct the PET images, which were then analyzed by comparing the reconstructed to true TC recovery coefficients. Simulated images with and without attenuation (AC) and scatter and random events included and rejected were analyzed.

The results showed that for strongly non-uniform attenuation and adequate statistics, very accurate attenuation, scatter and random corrections are needed to achieve accuracy better than 20% for most voxels, except close to regions with high gradient, where larger differences are seen. Insufficient scatter and random corrections lead to underestimation of the TC in regions with low attenuation. In such cases, tumors in the lung and close to the end of the axial FOV and with low statistics may not be seen. Reliable estimates of the quantification inaccuracy of 3D PET are needed if 3D PET is to be used for tumor segmentation and dose painting for radiation therapy.

I. INTRODUCTION

PET has the potential to serve two new roles in radiation oncology: (i) to supplement target volume delineation and (ii) to assist treatment planning in defining the biologically active and radiation resistant regions of the tumor. These two roles impose new requirements for PET, namely, to provide spatially and quantitatively accurate information of the tumor properties. The quantitative accuracy of PET has been measured for uniform phantoms containing simple geometrical volumes, but has never been studied for complex

Manuscript received November 16, 2007. This work was supported in part by a seed grant from the Department of Medical Physics at Memorial Sloan-Kettering Cancer Center and by the US National Cancer Institute grant No. CA059017-12.

All authors are with the Department of Medical Physics at Memorial Sloan-Kettering Cancer Center, New York, NY 10021, USA (telephone: 212-639-7126, e-mail: kirova@mskcc.org).

shape tumors and non-uniformly varying tracer concentration (TC) distributions.

In a previous study were compared the differences between segmented tumor volumes obtained with some of the currently used fixed threshold segmentation methods (without optimization for the particular scanner), in segmenting real tumors versus uniform activity cylinders and spheres [1]. The differences between the volumes obtained by the different methods were shown to be larger for the patient lesions than for the uniform objects by a factor of two or more. This indicates the larger uncertainty in segmenting real tumors compared to uniform lesions in uniform activity phantoms for which these methods were derived.

The activity distribution represented in a PET image differs from the actual tracer activity distribution due to physical limitations of the PET scanners, which are related to: position and direction dependent resolution and related partial volume effects, imperfect attenuation, random and sensitivity corrections, sampling effects, arc effects and the accuracy of the related depth of interaction correction, accuracy of the scatter coincidences correction, variable background activity, registration errors and tumor motion. This work is our first report from a project to determine the overall effect of the above factors for realistic TC and attenuation properties distributions. Here we investigate PET inaccuracy for TC and attenuation properties varying non-uniformly in one direction.

II. MATERIALS AND METHODS

A novel phantom arrangement consisting of thin parallel slabs was designed and simulated using GATE [2] in order to vary the TC and the attenuation properties in one direction. Such arrangement allows an efficient investigation of statistical effects by varying the number of averaged profiles, as well as the position and the orientation dependences of the quantification inaccuracy. Also an experimental phantom with the same specifications can be built for verification of the simulations. The phantom can be further modified to represent a 3D variation of the activity and the attenuation properties.

A schematic of the phantom is shown in Fig. 1. The core component is a plastic insert (a cube with side 12 cm), which is divided into slabs and which can be housed in different size phantom enclosures. The slabs (100 mm x 100 mm x 2 mm) are spaced with 0.127 mm polystyrene walls and may contain activity solution with different concentration and different attenuation properties. The slab insert was centered in a cylindrical water equivalent phantom enclosures with different

size filled with constant activity. The following four arrangements were simulated:

- (I) Activity and attenuation varying in the trans-axial direction, 30 cm diameter phantom enclosure;
- (II) Activity and attenuation varying in the trans-axial direction, 18 cm diameter phantom enclosure;
- (III) Activity varying in the trans-axial direction but uniform attenuation, 20 cm diameter phantom enclosure;
- (IV) Activity and attenuation varying in the axial direction, 30 cm diameter phantom enclosure;

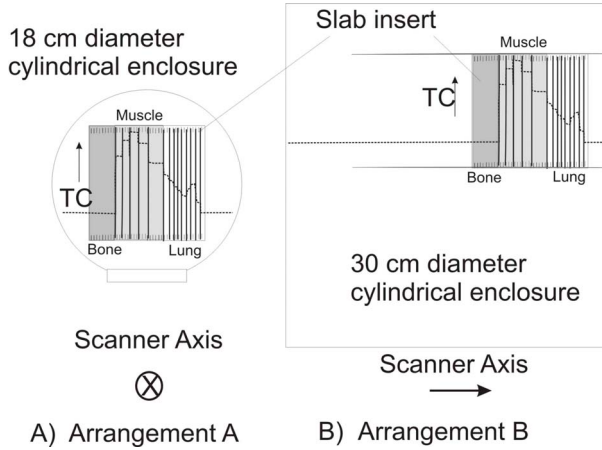


Fig. 1. A schematic of the slab phantom designed to allow arbitrary variations of the tracer concentration (TC) and the attenuation properties in one direction. An example TC profile is plotted with a dashed curve. The slab insert is placed inside cylinders with 18 cm and 30 cm diameter (A and B). In B the insert is also off center and rotated at 90 degrees as an illustration of a possible measurement arrangement. The slab walls are shown only at the points of change of the TC or of the attenuation properties.

The scanner model in 3D mode is based on the GE Discovery LS PET (Advance) scanner [3,4]. It contains 12,096 crystals ordered in 18 rings (56 modules, 6 blocks per module, 36 crystals per block). The events processing parameters used were: singles trigger 100 keV; energy window: 375 to 650 keV; crystal resolution: 20%; dead time: paralyzable 625 ns; Coincidences: timing window: 6.25 ns; minimum sector difference: 16.

The total activity in the phantoms was 135.009 MBq, 42.675 MBq, 53.809 MBq and 135.009 MBq for each of the arrangements respectively and 18 sec of coincidence simulations were analyzed. To eliminate the loss of count calibration from STIR (Software for Tomographic Image Reconstruction) [5], the reconstructed activity was scaled to the true activity in the broad uniform background regions, except for case IV for which no scaling was applied and the STIR output data was assumed to be in kilo counts.

To study the effect of the scatter and random coincidence events, the list mode data simulated by GATE was reanalyzed to generate two sets of sinograms: i) including all coincidences; ii) including only true coincidences, for which the scatter and random coincidences were rejected (SRR). Both sets were reconstructed using STIR with the 3D re-projection filtered back-projection (3DRPFBP) and the Ordered Subsets Expectation Maximization (OSMAPOS),

denoted in the figures as OSEM algorithms with a voxel size of 4.667 mm x 4.667 mm x 4.25 mm, 2 iterations, 28 subsets. Reconstructions were performed with and without attenuation correction corresponding to the simulated geometrical arrangement. A direct scanner geometry normalization correction, obtained from simulating a 30 cm radius cylindrical source, was applied.

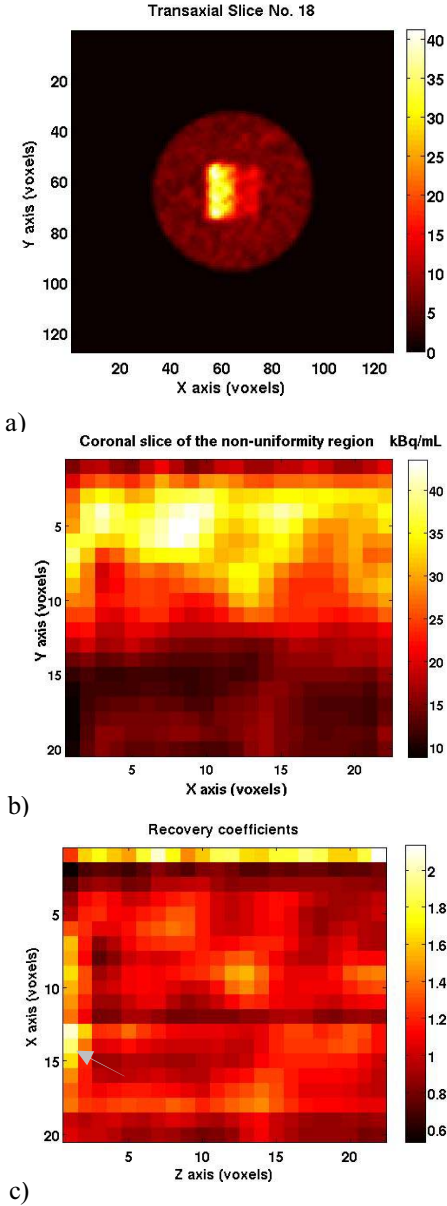


Fig. 2. Central transaxial slice obtained using MLEM (a), central coronal slice of the non-uniformity region only (b), and recovery coefficients for the slice (b) but with AC shifted with one slice (c) to illustrate attenuation correction registration error (arrow).

III. RESULTS

In Fig. 2. are shown images of slices and recovery coefficients for arrangement (I) above. A coronal slice of the non-uniformity region only (Fig. 2.b) illustrates how statistics affects the reconstructed activity distribution. For the recovery coefficient image (Fig. 2.c) the attenuation correction

image was shifted by one slice to illustrate the effect of incorrect registration of the attenuation correction, which is seen in the first axial position on the left. In Fig.2.c the overestimation in the top raw at minimum x reflects the inaccuracy in the high activity gradient bone region of the phantom.

For the case of single profiles (arrangement I)), which are with poor statistics (Fig. 3 a,b), the recovery coefficient is within a factor of 2 only for the OSMAPOL (OSEM) reconstructed images with exact attenuation and scatter and random corrections. For the high statistics averaged profiles both the fully corrected OSEM and 3DRP are accurate within $\sim 20\%$, except close to the strong TC gradient bone region, where inaccuracy greater than 50% is observed (Fig. 3 c,d). Non-attenuation corrected and non scatter and random rejected images exhibit over- and under-response in the low attenuation region for this arrangement (I).

Decreasing the phantom diameter to 18 cm (arrangement II, Fig. 4 a,b) practically eliminates the under-response in the lung area for the images containing scatter and random. Simulations using small phantom diameter and uniform attenuation (arrangement III, Fig. 4 c,d) show that even without very accurate scatter and attenuation correction one can get accuracy within $\sim 20\%$ for such simpler cases. Our preliminary results show that rotating the non-uniformity slab along the scanner axis (arrangement IV) leads to severe inaccuracies, specifically underestimation in the lung region (Fig. 4 e,f). The reasons for the last result are currently being investigated.

IV. DISCUSSION

The slab phantom design showed the following advantages over other phantoms [6,7] used to obtain non-uniform activity distributions: i) The 1D implementation allows obtaining both low and high statistics activity profiles by varying the number of averaged identical profiles; ii) Rotating or relocating the 1D phantom in different size enclosures allows accurate testing of the orientation and positional dependences of PET's quantification accuracy; iii) The phantom can be manufactured and can be extended to 3D by varying the activity and the attenuation properties between and within the slabs. The latter can be obtained by preloading each slab cell with material with variable attenuation properties and computer generated shapes similarly to [7] prior to pouring the same activity solution in all cells.

Our future efforts will be concentrated in repeating the above analysis for reconstructions performed using the vendor's software and experimental validation of the simulations for 2D and 3D PET. Further we will investigate a larger variety of activity distributions corresponding to typical patient tumors both through simulations and experiments. Finally we will seek correction and optimization strategies to improve PET quantification accuracy for such cases.

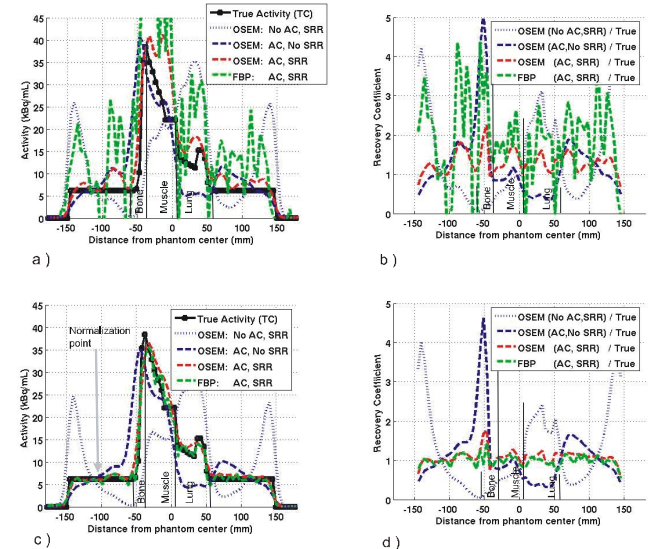


Fig. 3. Single (a, b) and averaged (c, d) activity profiles and recovery coefficients across the non-uniform slab for arrangement (I) centered axially inside the slab insert and the scanner. The profiles are normalized at the indicated point in the background region. The notations are: OSEM = OSMAPOL, FBP = 3DRPFBP, AC = attenuation correction, SRR = Scatter and Random Rejection.

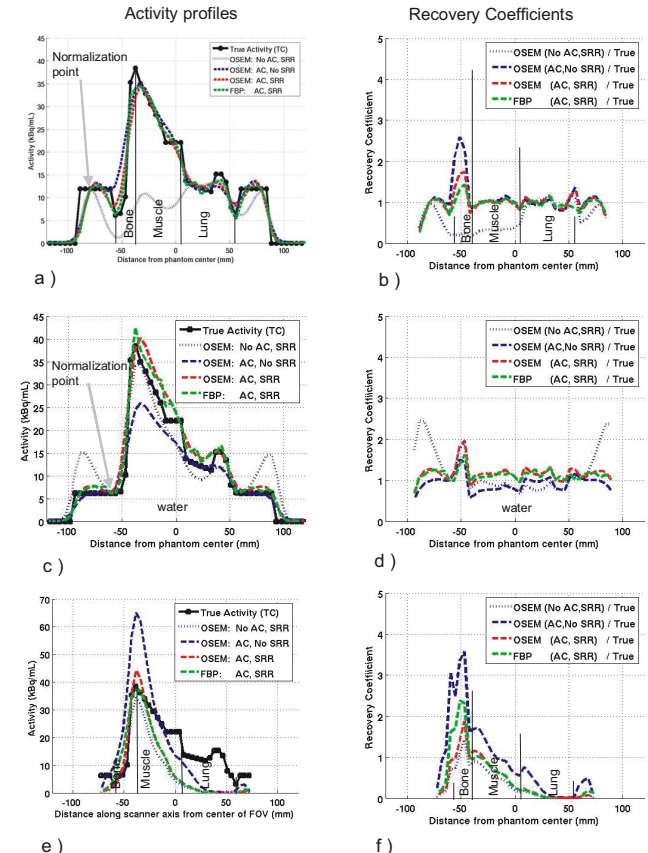


Fig. 4. Activity profiles and recovery coefficients for phantom configurations II (a,b): 18 cm diameter enclosure; III (c,d): 20 cm diameter enclosure and uniform attenuation; and IV (e,f): activity varying in the axial direction, 30 cm diameter enclosure. The notations are the same as in Fig. 3.

V. CONCLUSION

Monte Carlo simulations of the designed parallel slabs phantom allowed to model both variable activity and attenuation in one direction and proved to be an effective model for studying PET quantification inaccuracy. The phantom allows investigating statistic effects by varying the number of averaged profiles, as well as investigating the position and the orientation dependences of the quantification inaccuracy.

For the case of strongly non-uniform attenuation, highly accurate attenuation, scatter and random corrections are needed to ensure activity recovery accuracy better than $\sim 25\%$ throughout most of the image. However, even in this case the local quantification inaccuracy of 3D PET can exceed 50% for voxels close to strong activity gradients and strong attenuation. Miss-registration of the AC with 1 slice can cause inaccuracies larger than a factor of 2.

Insufficient Scatter and Random Corrections may lead to underestimating the tracer concentration in low attenuation regions. Our preliminary results show that tumors in the lung with low statistics and close to the end of the axial field of view may not be seen.

REFERENCES

- [1] A. S. Kirov, C Danford, C Schmidlein, E Yorke, J Yahalom, H Kalaigian, Y Hu, S Larson, J Humm, H Amols "Inaccuracy of Fixed Threshold Segmentation for PET", Presented at the 48-th Annual Meeting of the AAPM, Orlando, FL, July 30-August 3, 2006, *Med. Phys.* 33, p 2039, 2006
- [2] S. Jan, G. Santin, D. Strul, K. Assi, D. Autret, S. Avner, R. Barbier, M. Bardi, P. Bloomfield, D. Brasse, V. Breton, P. Bruyndonckx, I. Buvat, A.F.Chatzioannou, Y. Choi, Y.H. Chung, C. Comtat, D. Donnarieix, L. Ferrer, S.J. Glick, C. Groselle, S. Kerhoas-Cavata, A.S. Kirov, V. Kohli, M. Koole, M. Krieguer, D.J. van der Laan, F. Lamare, G. Langeron, C. Lartizien, D. Lazaro, M.C. Maas, L. Maigne, F. Mayet, F. Melot, C. Merheb, C. Morel, E. Pennacchio, J. Perez, U. Pietrzky, F.R. Rannou, M. Rey, D.R. Schaart, C.R. Schmidlein, L. Simon, T.Y. Song, S. Staelens, J.-M. Vieira, D. Visvikis, R. Van de Walle, E. Wie, "GATE – Geant4 Application for Tomographic Emission: a simulation toolkit for PET and SPECT", *Phys. Med. Biol.*, vol. 49, pp. 4543-4561, 2004
- [3] C R Schmidlein, A S Kirov, Bidaut L, Nehmeh S, Erdi Y, Ganin A, Stearns C W, McDaniel D L, Humm J, and Amols H, "Validation of GATE Monte Carlo simulations of the GE Advance/Discovery LS PET Scanners, *Med. Phys.*, vol. 33, no.1, pp. 198-208, Jan. 2006.
- [4] C.R. Schmidlein, A.S Kirov, S.A. Nehmeh, L.M. Bidaut, Y.E. Erdi, K.A. Hamacher, J.L. Humm, H.I. Amols, "Validation of GATE Monte Carlo Simulations of the Noise Equivalent Count Rate and Image Quality for a GE Discovery LS PET Scanner", Presented at the 47-th Annual Meeting of the AAPM, Seattle, July 2005, *Med. Phys.*, vol. 32, no. 6, p.1900, June 2005.
- [5] K. Thielemans, D. Sauge, C. Labbe, C. Morel, M.Jacobson, A. Zverovich, "STIR Software for Tomographic Image Reconstruction: User's Guide, Version 1.4. Hammersmith Imanet, <http://stir/irsl.org/documaentation/STIR-UsersGuid.pdf>, November 2004.
- [6] H. El-Ali, M. Ljungberg , S. E. Strand, J. Palmer, L. Malmgren, J. Nilsson "Calibration of a radioactive ink-based stack phantom and its applications in nuclear medicine." *Cancer Biother Radiopharm*, vol. 18, no. 2, 201-7, 2003.
- [7] F. P. DiFilippo, J. P. Price, D. N. Kelsch, R. F. Music, "Porous phantoms for PET and SPECT performance evaluation and quality assurance." *Med. Phys.* Vol. 31, no. 5, pp. 1183-94, May 2004